Positioning high-throughput CETSA in early drug discovery through screening against B-Raf and PARP1

Joseph Shaw[1], Ian Dale[1], Paul Hemsley[1], Lindsey Leach[2], Nancy Dekki[5] Jonathan P Orme[1], Verity Talbot[3], Ana J Narvaez[3], Michal Bista[4], Daniel Martinez Molina[5], Michael Dabrowski[5], Martin J Main[1#], Davide Gianni[1].

[1]Discovery Biology, Discovery Sciences, IMED Biotech Unit, AstraZeneca, Cambridge, UK.
[2]Hit Discovery, Discovery Sciences, IMED Biotech Unit, AstraZeneca, Alderley Park, UK.
[3]Mechanistic Biology & Profiling, Discovery Sciences, IMED Biotech Unit, AstraZeneca, Cambridge, UK.
[4]Structure, Biophysics & Fragment Based Lead Generation, Discovery Sciences, IMED Biotech Unit, AstraZeneca, Cambridge, UK.
[5]Pelago Bioscience AB, 171 65 Solna, Sweden.

[#]Current address: Medicines Discovery Catapult, Mereside, Alderley Park, UK.

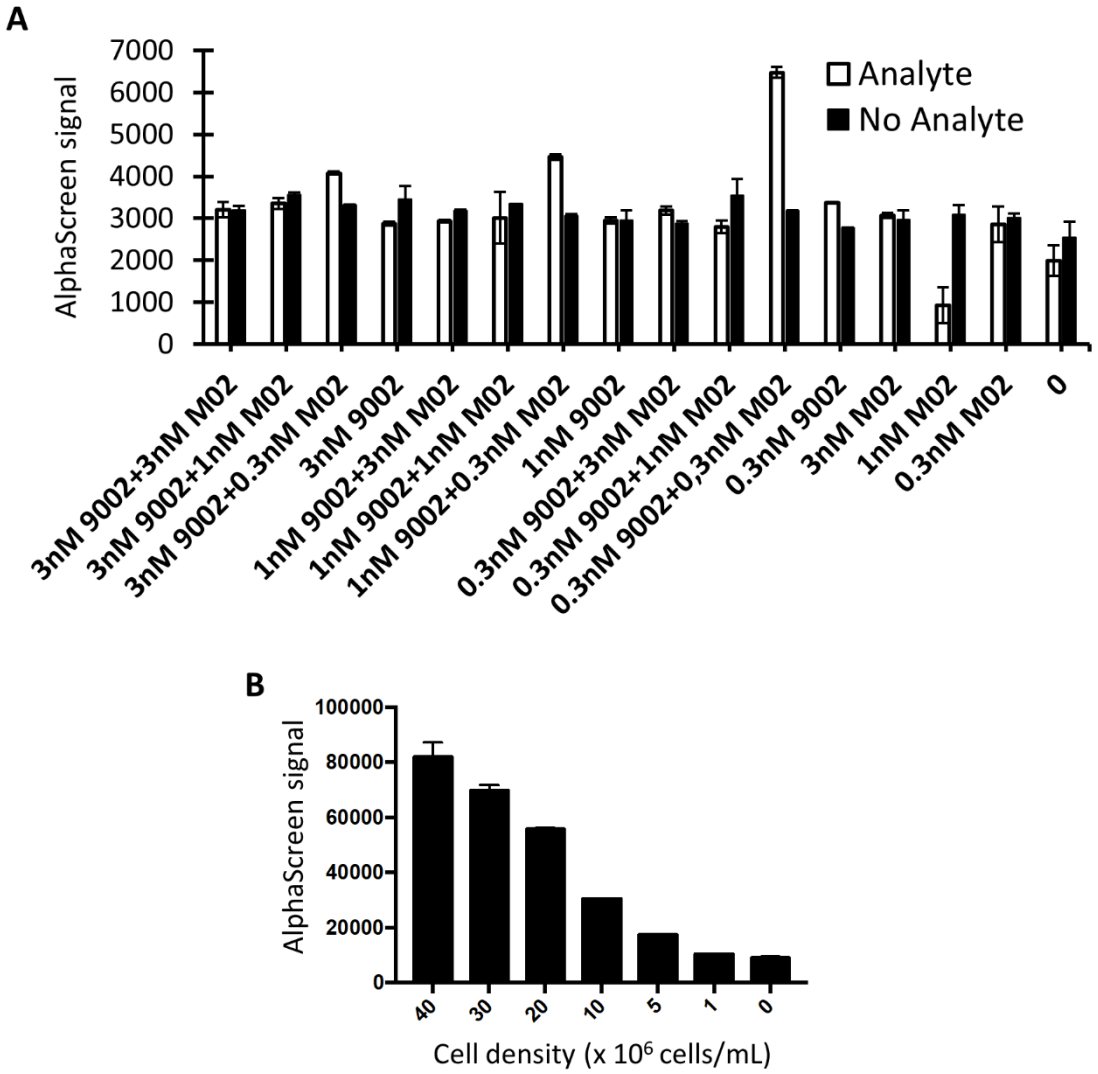

Supplementary Figure 1. Optimisation of an antibody pair to enable quantification of thermostable B-Raf by AlphaScreen®. (**A**) The antibody pair sc-9002 rabbit anti-B-Raf (9002) and H00000673-M02 mouse anti-B-Raf (M02) were tested at various indicated final concentrations in the presence (white) or absence (black) of a source of B-Raf, A549 cell lysates. A final antibody concentration of 0.3 nM sc-9002 and 0.3 nM H00000673-M02 was selected. Data are the mean ± span of n=2. (**B**) Optimal concentrations of anti-B-Raf antibodies were tested against various cell densities of A549 cells. A density of 15 x 10^6 cells/mL was within the linear range and selected. Data are the mean ± span of n=2.

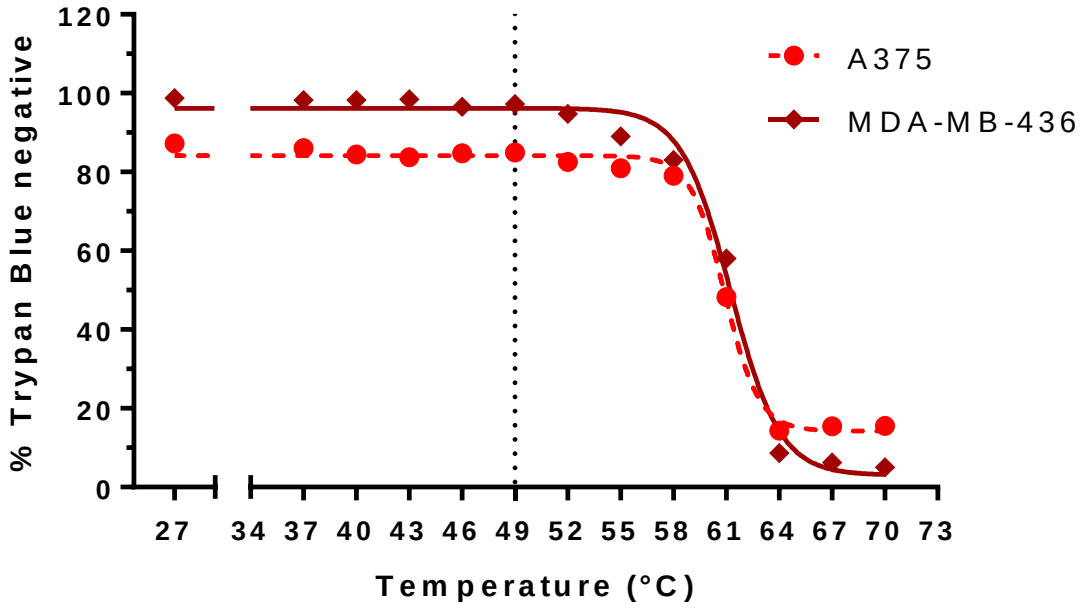

Supplementary Figure 2. Impact of the CETSA heatshock on membrane integrity for cell lines used within this study. A 3 minute heatshock at the indicated temperature followed by a 1 minute cool at 25˚C was applied to 1 x 10^6 cells in 100 µL complete media. Heat-shocked cells were added to 400 µL media, mixed 1:1 with Trypan Blue and live/dead cells quantified using a Vi-Cell XR cell viability analyzer. Data are the average counts from 50 fields of view from one technical repeat. For both A375 and MDA-MB-436 cell lines, membranes remained viable (Trypan Blue negative) up to a heat shock of 58˚C, well above the heatshock temperature used for CETSA experiments (49˚C, dashed line).

AZ12823138

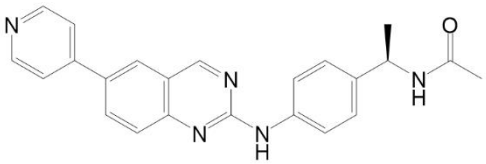

Cmpd **2**

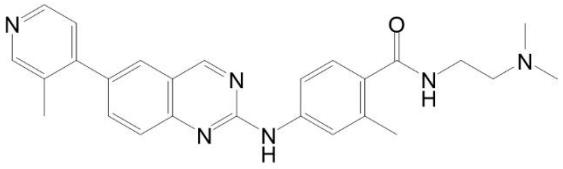

Cmpd **3**

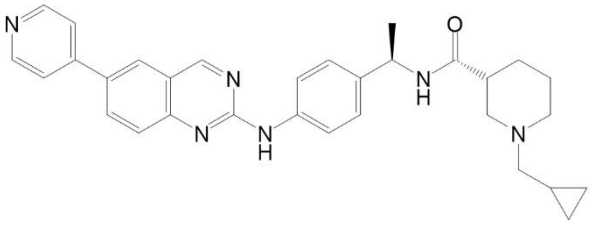

Supplementary Figure 3. Chemical structures of AstraZeneca B-Raf inhibitors identified from CETSA HT screening of a diverse kinase library. AZ12823138 and structurally related compounds **2** and **3** have previously been identified as Raf inhibitors with activity against B-Raf.

Dabrafenib

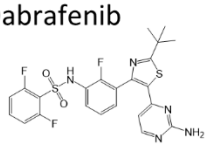

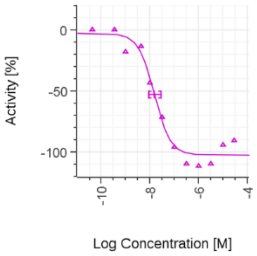

LY3009120

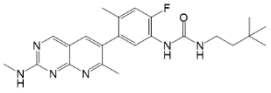

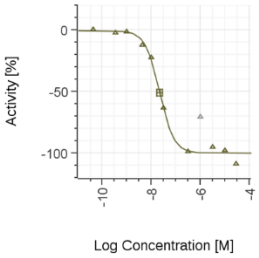

AZ628

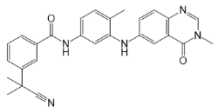

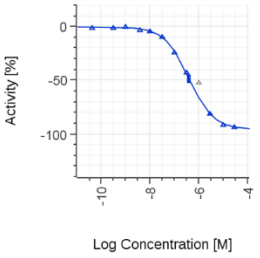

Vemurafenib

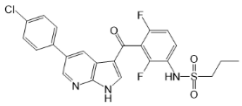

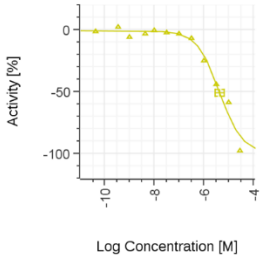

PLX4720

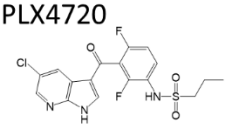

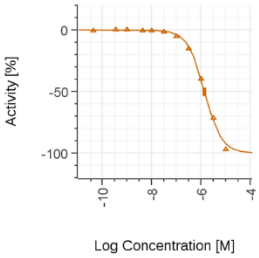

Vemurafenib analogue

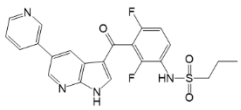

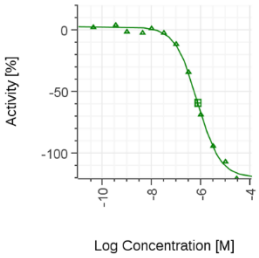

AZ12823138

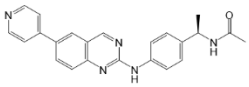

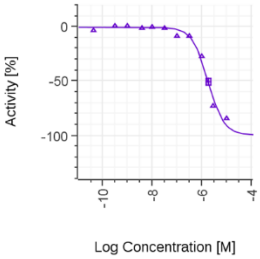

Cmpd **4**

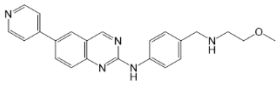

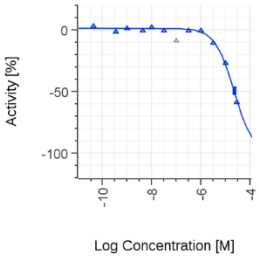

PLX5568

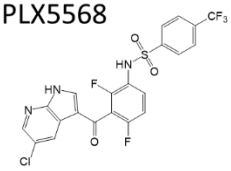

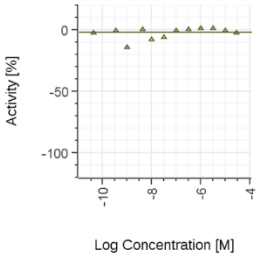

CH-5126766

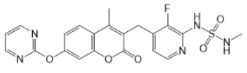

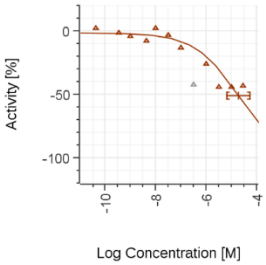

Selumetinib

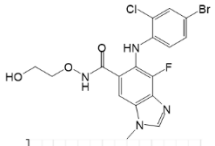

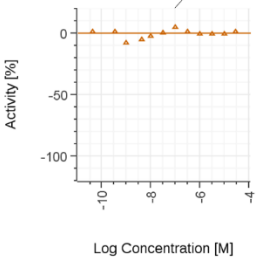

PD325901

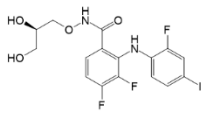

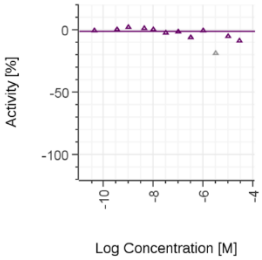

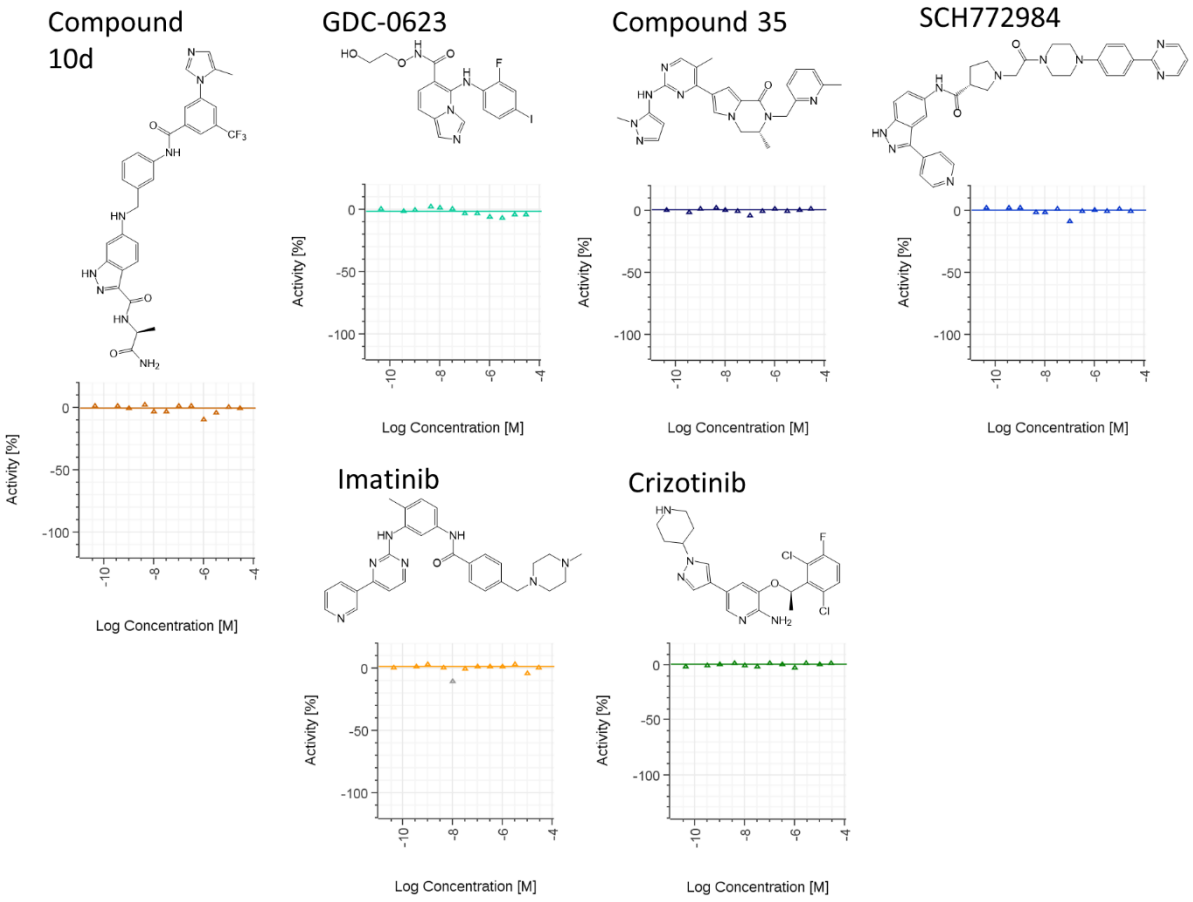

Supplementary Figure 4. Representative plots for $ITDRF_{CETSA}$ data reported in Table 1. Potency (pEC_{50}) of intracellular B-Raf target engagement for indicated compounds was determined using Genedata Screener and reported in Table 1. Data was normalised to Dabrafenib control (-100 % Activity). Data shows n=1 replicates and is representative of ≥ 3 technical repeats.

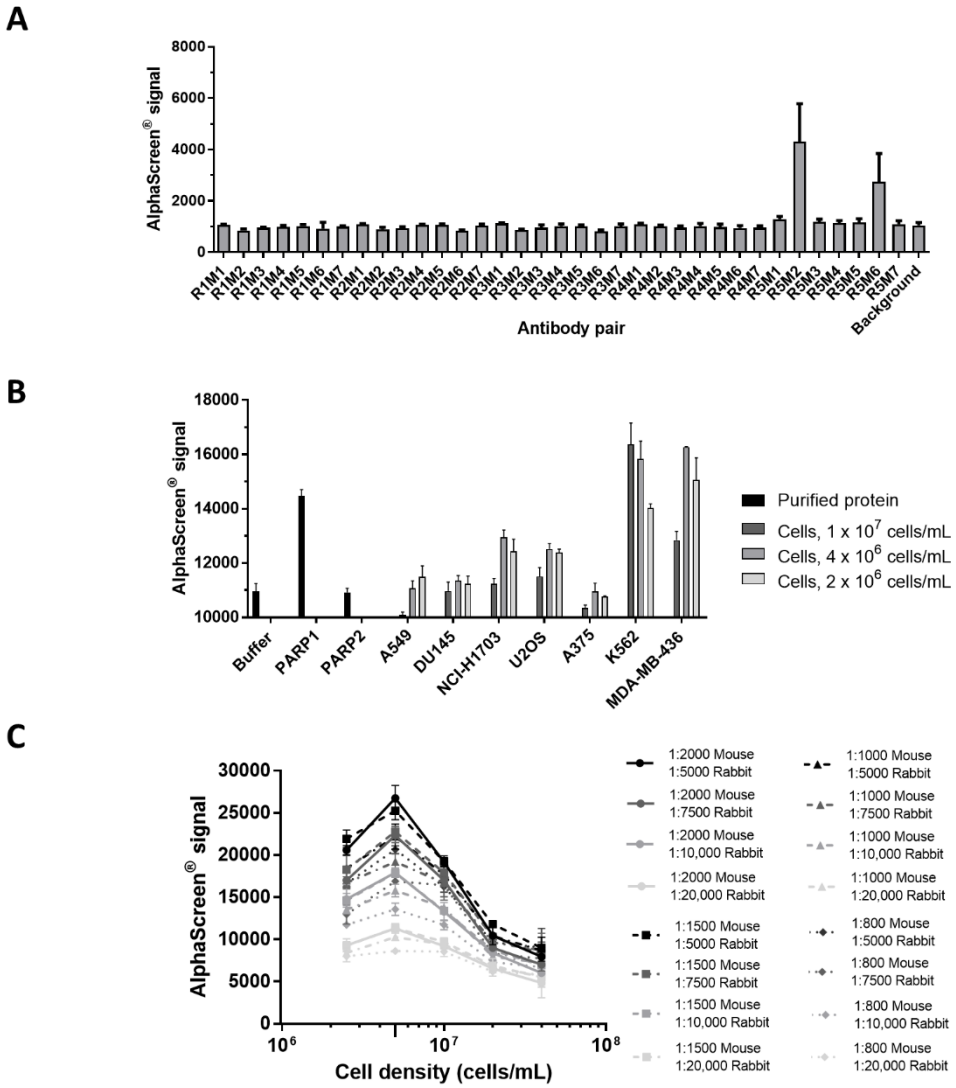

Supplementary Figure 5. Optimisation of an antibody pair to enable quantification of thermostable PARP1 by AlphaScreen®. (**A**) Panels of rabbit anti-PARP1 and mouse anti-PARP1 antibodies were screened for productive AlphaScreen® signal in the presence of MDA-MB-436 cell lysates, anti-mouse AlphaScreen® donor and anti-rabbit AlphaScreen® acceptor. R1 – ThermoScientific PA5-13386; R2 – ThermoScientific PA5-27219; R3 – Proteintech 13371-1-AP; R4 – Enzo ALX-210-302-R100; R5 – Cell Signalling Technologies 9542S; M1 – BD Pharmingen 51-9000017; M2 – Sigma WH0000142M; M3 – Sigma C-2-10; M4 – MerckMillipore MABE18; M5 – Abcam ab177529; M6 – BD Pharmingen 556494; M7 – Invitrogen A21969. The antibody pair R5M2 was selected. (**B**) The R5M2 antibody pair selectively quantifies PARP1 in a variety of cell lines. Purified recombinant full-length PARP1 or PARP2 protein was used to assess the PARP1-selectivity of the AlphaScreen® signal. The AlphaScreen® signal was assessed from lysates of a range of cell lines prepared at indicated densities. (**C**) Optimisation of MDA-MB-436 cell density and mouse anti-PARP1 and rabbit anti-PARP1 antibody dilutions for optimal AlphaScreen® signal. The optimal cell seeding

density was 4 x 10^6 cells/mL (4 x 10^4 cells/well). Optimal antibody dilutions were selected as 1:2000 Sigma WH0000142M mouse anti-PARP1 and 1:5000 CST 9542S rabbit anti-PARP1 prior to addition to the plate.

A

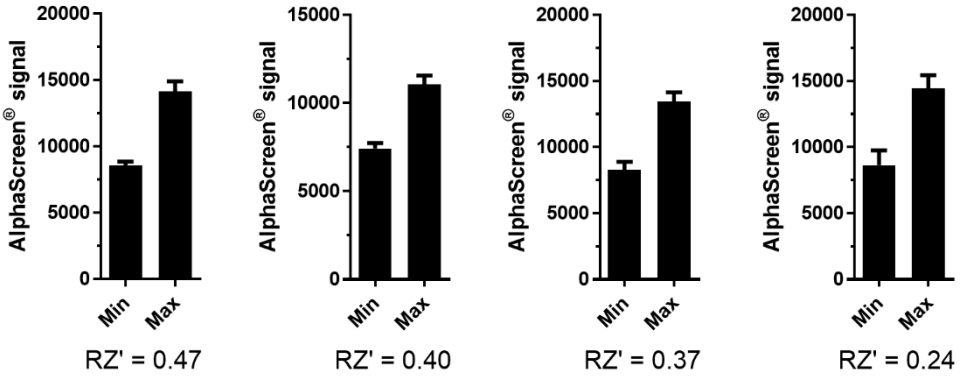

B

	Max %CV	RZ'	Signal:noise
n=1	5.50	0.468	1.65
n=2	4.52	0.395	1.49
n=3	5.22	0.370	1.63
n=4	6.94	0.240	1.67

C

	n=1	n=2	n=3	n=4
Olaparib pEC_{50}	8.06	8.12	8.16	7.94
Rucaparib pEC_{50}	7.49	7.04	-	7.30
NMS-P118 pEC_{50}	6.58	6.35	6.28	6.52

Supplementary Figure 6. PARP1 CETSA HT assay performance. (**A**) Plate Max-Min controls showing thermostable PARP1 quantified from four technical repeats of in-cell CETSA HT experiments. Min = 0.3% DMSO, Max = 30 µM Olaparib. Calculated Robust Z-factor (RZ') is shown. Data are the mean ± standard deviation of n=12. (**B**) Tabulated assay performance parameters from data reported in A. RZ' and %CV were considered acceptable, although signal-to-noise was < 2. (**C**) Calculated $ITDRF_{CETSA}$ pEC_{50} determined with a 49°C heat shock across several technical repeats for three tool compounds. Determined pEC_{50} for in-cell target engagement was reproducible.

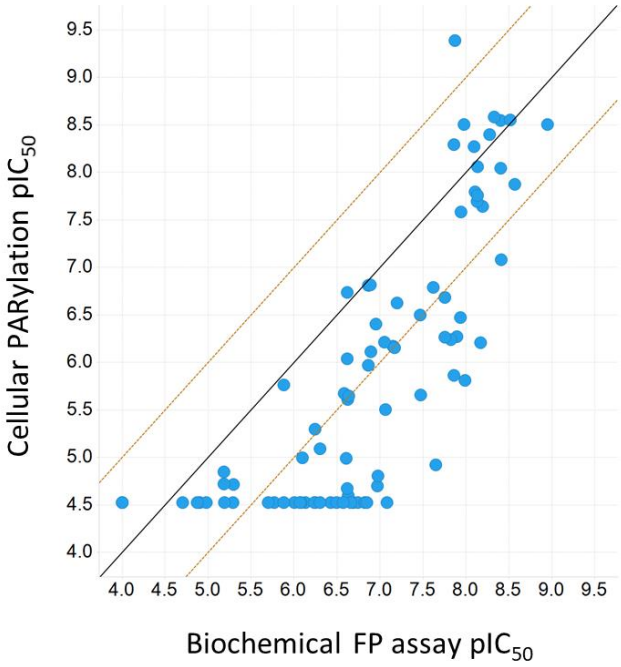

Supplementary Figure 7. Comparison of PARP inhibitor potency between a biochemical binding assay and an alternative cell assay. pIC_{50} determined in the cellular PARylation assay plotted against pIC_{50} determined in the biochemical FP assay for 85 PARP inhibitors. The solid line shows a 1:1 correlation, and dashed lines represent a 1 log_{10} shift in potency.

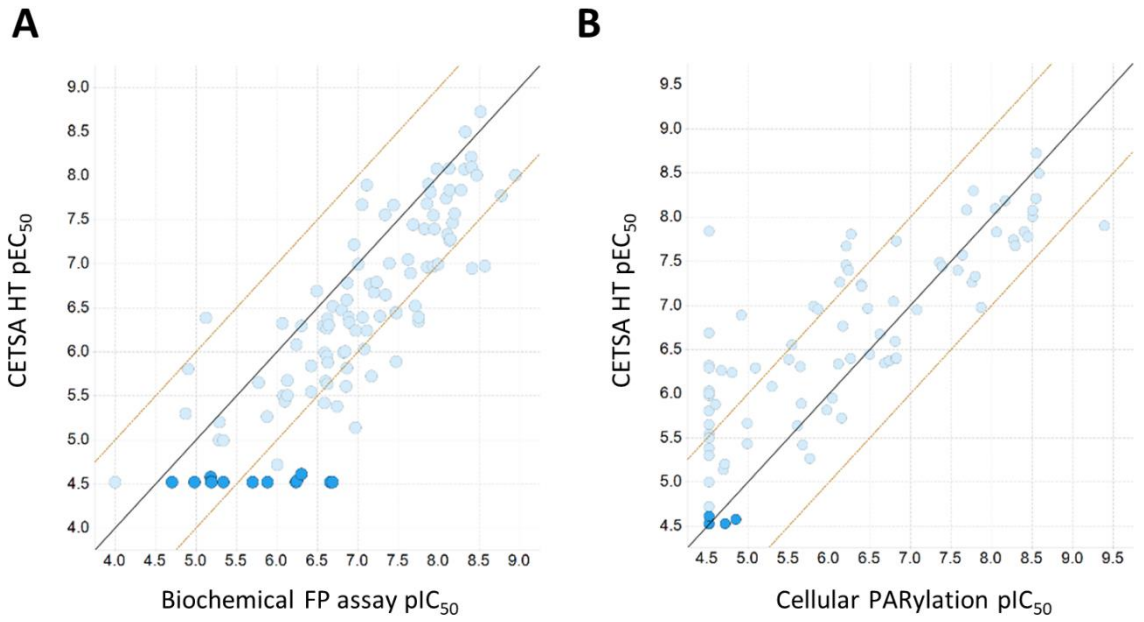

Supplementary Figure 8. Analysis of compounds showing discrepancy between the Biochemical FP assay and CETSA HT. (**A**) Comparison of compound activity in the Biochemical FP assay and CETSA HT. Highlighted are 13 compounds which were active in the Biochemical FP assay but inactive in CETSA HT. (**B**) The same 13 compounds highlighted in a comparison of CETSA HT and an alternative cellular assay measuring PARylation. All 13 compounds were inactive in both cell assays, indicating a lack of cellular permeability as a cause of inactivity. The solid line shows a 1:1 correlation, and dashed lines represent a 1 $\log_{10}$ shift in potency.

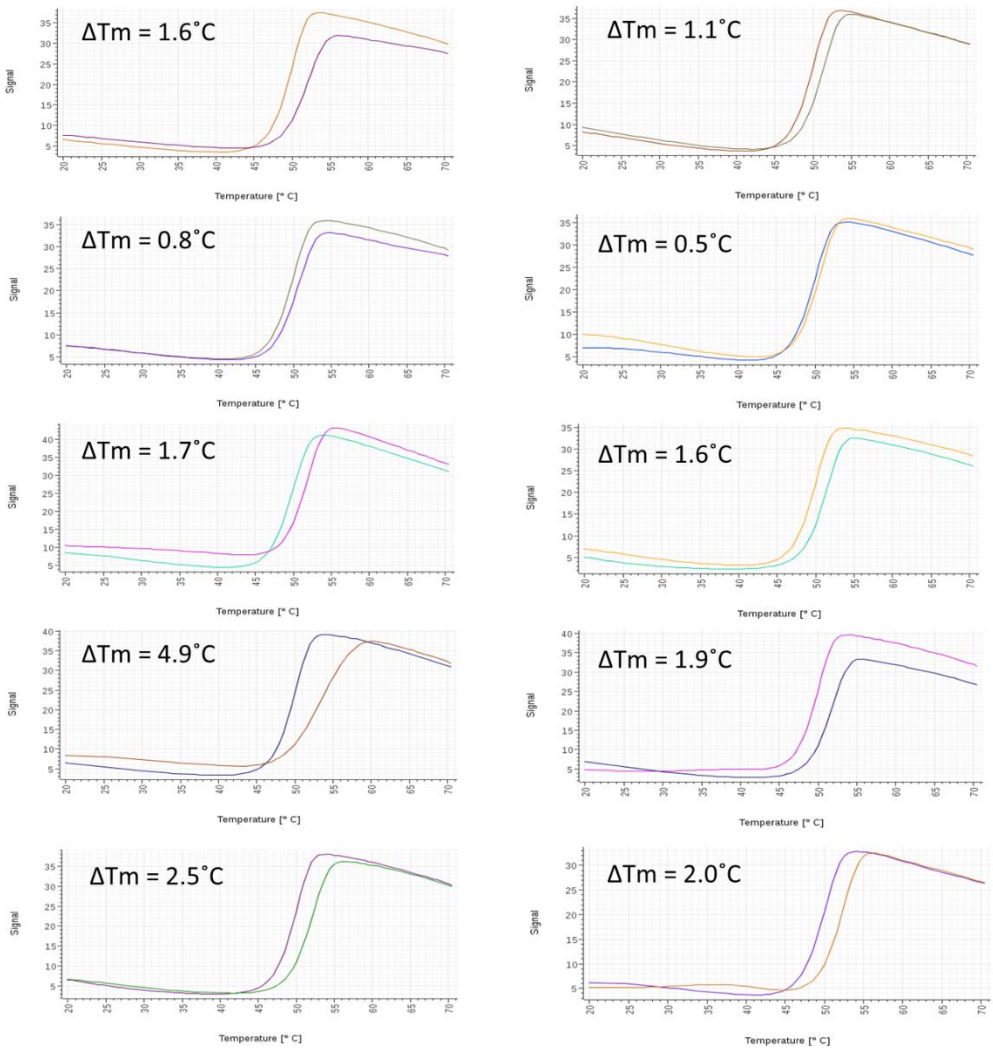

Supplementary Figure 9. Testing of compounds showing discrepancy between the Biochemical FP assay and CETSA HT for a thermal shift by differential scanning fluorimetry. Thermal melt curves are shown for 10 compounds which were active in the FP assay but inactive in CETSA HT (highlighted in Supplementary Figure 8A). Compounds were profiled at a test concentration of 30 µM. Thermal shifts were observed relative to DMSO control, with most compounds showing a ~2˚C ΔTm similar to the thermal shift observed by CETSA HT (Figure 2A).

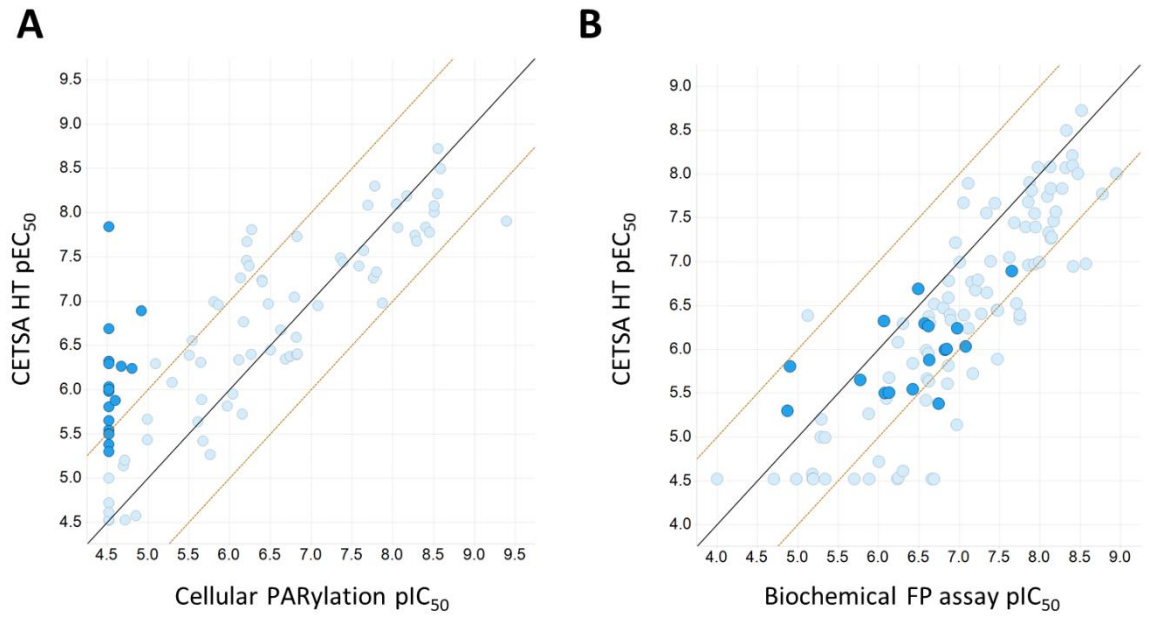

Supplementary Figure 10. Analysis of compounds showing discrepancy between the CETSA HT and the Cellular PARylation assay. (**A**) Comparison of compound activity in CETSA HT and the Cellular PARylation assay. Highlighted are 19 compounds which were active in CETSA HT but inactive in the functional PARylation assay. (**B**) The same 19 compounds highlighted in a comparison of CETSA HT and the Biochemical FP assay. All 19 compounds show similar potencies of binding by both CETSA HT and the Biochemical FP assay, indicating the CETSA HT assay is informing on true binders. The solid line shows a 1:1 correlation, and dashed lines represent a 1 $\log_{10}$ shift in potency.